Pulse-stacked cavity ring-down spectroscopy

E. R. Crosson, P. Haar, G. A. Marcus, and H. A. Schwettman
Department of Physics, Stanford FEL Center, Stanford University, Stanford, California 94305-4085

B. A. Paldus, T. G. Spence, and R. N. Zare[a)]
Department of Chemistry, Stanford University, Stanford, California 94305-5080

(Received 22 September 1998; accepted for publication 23 October 1998)

Pulse stacking, or synchronous pumping, is a novel approach that offers important advantages in cavity ring-down spectroscopy. Using an ultrashort pulse, high repetition rate laser source we have shown that it is possible to resonantly stack pulses in a high finesse cavity, significantly enhancing the decay wave forms obtained when the laser source is abruptly terminated. We have achieved signal-to-noise ratio improvements of several orders of magnitude compared to single pulse injection systems, demonstrating a sensitivity of 2×10^{-9} cm^{-1} at 5.38 μm. © *1999 American Institute of Physics.* [S0034-6748(99)04801-7]

I. INTRODUCTION

Cavity ring-down spectroscopy (CRDS) is a general, high-sensitivity technique for measuring absorption which has been applied primarily to studies of species that are either very dilute or very weakly absorbing.[1] In CRDS, light from a laser source is injected into a high finesse optical resonator, called the ring-down cavity (RDC), that encloses the sample of interest. When the light source is interrupted, light trapped inside the optical resonator decays exponentially owing to finite resonator losses and absorption by the sample. An absorption spectrum of the sample species is obtained by measuring the decay rate, the inverse of the decay time constant, τ, as a function of wavelength, and subtracting the background decay rate for the empty resonator.[2] By using high reflectivity mirrors, resonator losses can be minimized, thereby increasing sensitivity to sample absorption. The method provides a very long effective pathlength for sample absorption and is insensitive to amplitude fluctuations of the laser source.[3–6]

CRDS has been performed using both pulsed[3–6] and continuous wave (CW) laser sources.[7–9] Pulsed CRDS (P-CRDS) is the most common method of operation and the most straightforward to implement. The technique, however, suffers from important limitations. Because pulse duration is typically less than several RDC roundtrip times, no significant energy buildup occurs in the optical resonator and thus the detected signal at the cavity output is severely attenuated. For mirror transmission of 500 parts per million (ppm), the input signal intensity will be reduced 2.5×10^{-7} times by passing through the RDC. This attenuation produces weak output signals with inferior signal-to-noise characteristics. Furthermore, many pulsed laser sources have repetition rates lower than 1 kHz, which preclude extensive averaging to improve the signal-to-noise ratio. Finally, for a transform-limited laser source, the spectral width of a 10 ns optical pulse is 44 MHz. Thus, to achieve better resolution, spectral analysis of the beam emerging from the RDC is required.[10]

An alternative method of operation in CRDS is to use CW laser sources (CW-CRDS). The major difficulty in this method is achieving regular and reproducible overlap between a longitudinal cavity mode and the laser line.[7,8,11,12] When this is accomplished, however, a large intracavity field is generated, and cavity throughput is only limited by the ratio of the cavity and laser linewidths. For typical midinfrared experiments using 500 ppm mirrors, and a 2 m long RDC, the attenuation of the input signal varies from unity for a CW optical parametric oscillator[13] to 5×10^{-3} for a CW quantum cascade laser,[14,15] a significant improvement over the P-CRDS case. In CW-CRDS, the laser is switched off using an external acousto-optic modulator, allowing repetition rates up to tens of kilohertz, limited only by the RDC buildup and ring-down time constants.[7,12] In contrast to P-CRDS,[16] a CW laser and RDC can be matched to the appropriate longitudinal and transverse mode, thereby eliminating excess noise in the decay wave forms. Finally, because only a single RDC mode is excited, the resolution of the CW-CRDS technique is limited, at least in principle, only by the RDC linewidth, which is typically on the order of several tens of kilohertz.

In this article we describe a novel approach to P-CRDS in which a train of coherent, ultrashort pulses from a high repetition rate laser are stacked to achieve high throughput, as illustrated in Fig. 1.[17,18] In pulse-stacked CRDS (PS-CRDS) resonant buildup of the cavity field is achieved, but without a limited throughput caused by the cavity linewidth. The throughput, in principle, is unity. In PS-CRDS the stacked pulse is spectrally broad, but it is possible to recover resolution by analysis of the transmitted beam, using either a dispersive element and an array detector or a Fourier-transform spectrometer. As in CW-CRDS, the repetition rate is limited to a few tens of kilohertz by the resonator buildup and ring-down time constants. In this first demonstration of PS-CRDS, a high repetition rate (11.8 MHz) infrared free electron laser (FEL) beam at the Stanford Picosecond FEL Center was used. The exceptional beam quality and stability of the FEL and its ease of tuning over a wide spectral range

[a)]Electronic mail: zare@stanford.edu

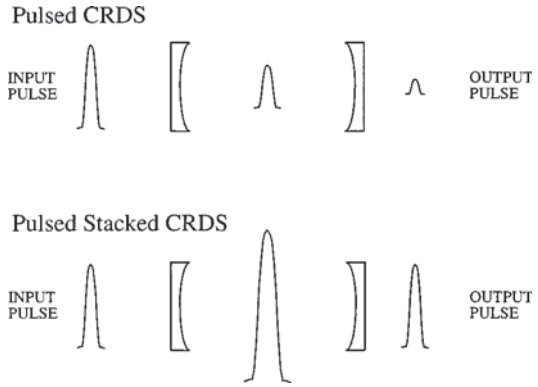

FIG. 1. Illustration of the difference between pulsed CRDS and pulse-stacked CRDS. For cavity mirrors with 500 ppm transmission, the transmitted energy for pulsed CRDS is $(2.5\times10^{-7})U_{\mathrm{inc}}$. For pulse-stacked CRDS the pulse energy inside the RDC is $(2\times10^{3})U_{\mathrm{inc}}$ and the transmitted energy is U_{inc}.

make it well suited to PS-CRDS. The principles of pulse stacking, validated in previous experiments[19–22] with the Stanford FEL, are discussed in this article. In Sec. III, relevant, details of laser performance, mode matching, beam steering, cavity optics, and the monochromator used for spectral analysis are described. To illustrate detection sensitivity and other system capabilities achieved, PS-CRDS noise statistics and simple spectral data are presented. Finally, potential applications of PS-CRDS are briefly discussed.

II. PULSE STACKING IN A RING-DOWN CAVITY

It is possible to achieve high throughput in a RDC by stacking pulses from a high repetition rate laser. The conditions for efficient pulse stacking can be stated simply: The external laser beam must be coupled into the cavity along its optical axis; the beam transverse mode must be matched to the cavity transverse mode; and the cavity round-trip path length must equal to a multiple of the spatial separation of individual pulses in the external laser pulse train.

In addition, coherence of the external laser pulse train must extend over a time equal to the cavity filling time and dispersion in the RDC must be small. First we present a brief discussion of the principles of pulse stacking as applied to PS-CRDS; then we discuss the practical aspects of satisfying the above criteria for pulse stacking.

A. General principles

For an empty ring-down cavity formed from two identical mirrors with field transmission and reflection coefficients, t and r, the stacked field in the cavity, E_{cav}, after n pulses each of field amplitude, E_{inc}, can be written[23]

$$\begin{aligned} E_{\mathrm{cav}} &= tE_{\mathrm{inc}} + t(r^2)E_{\mathrm{inc}} + t(r^2)^2E_{\mathrm{inc}} \\ &\quad + t(r^2)^3E_{\mathrm{inc}} + \cdots + t(r^2)^nE_{\mathrm{inc}} \\ &= tE_{\mathrm{inc}}\,\frac{1-r^{2(n+1)}}{1-r^2}. \end{aligned} \tag{1}$$

After an arbitrarily large number of pulses have entered the cavity, the energy of the stacked pulses, U_{cav}, reaches an asymptotic value

$$U_{\mathrm{cav}} = \frac{t^2U_{\mathrm{inc}}}{(1-r^2)^2}, \tag{2}$$

where U_{inc} is the incident pulse energy. If the incident pulse train is abruptly terminated, the energy in the cavity decays exponentially with a characteristic time constant, $\tau = (2L/c)/(1-R)$ where $2L$ is the cavity round-trip length. The optical resonator can also be characterized by its finesse, F, which is related to reflectivity, R, by $F = \pi\sqrt{R}/1-R \approx \pi/1-R \approx \pi/\ln(1/R)$, and is the ratio of the cavity mode linewidth full width at half maximum (FWHM) to the cavity free spectral range. In terms of the cavity finesse and the power transmission and reflection coefficients, $T = t^2$ and $R = r^2$, respectively, the asymptotic stacked energy is

$$U_{\mathrm{cav}} = \frac{TU_{\mathrm{inc}}}{(1-R)^2} = \frac{TU_{\mathrm{inc}}}{(1-e^{-\pi/F})^2}. \tag{3}$$

For a typical RDC, the finesse is large and the stacked energy is approximately

$$U_{\mathrm{cav}} = TF^2U_{\mathrm{inc}}/\pi^2. \tag{4}$$

For mirrors with 500 ppm power transmission, and negligible scattering and attenuation, the cavity finesse is 2000π, and the stacked energy is 2000 times the incident pulse energy. Of particular relevance to CRDS is the energy throughput from source to detector. The energy of the pulse coupled out of the RDC and detected is 5×10^{-4} times the stacked pulse energy (2 000 times U_{inc}) and thus is equal to the incident pulse energy. In principle, for perfect stacking, the throughput is unity by an argument almost identical to that used for CW-CRDS, and the RDC appears transparent to the incident radiation.

It is instructive to compare short-pulse PS-CRDS and CW-CRDS in terms of stored energy and peak intensity. Consider, therefore, a 1 W, 100 MHz train of 2 ps pulses and a 1 W, CW beam of 5.0 μm light. Assume a confocal cavity having a length L of 1.50 m and mirrors with $T = 5\times10^{-4}$. For the PS-CRDS case, U_{inc} is 10 nJ per pulse, and U_{cav} is 20 μJ from Eq. (4). The light intensity at the waist in the RDC is given by

$$I_{\mathrm{waist}} = \frac{U_{\mathrm{cav}}/\Delta t_p}{\pi w_0^2}, \tag{5}$$

where Δt_p is pulse duration, and $w_0 = \sqrt{(\lambda L)/(2\pi)}$ for the TEM_{00} transverse mode of the confocal optical resonator. I_{waist} therefore equals 2.7×10^{8} W/cm^2. For the CW-CRDS case, the energy stored in the RDC is

$$U_{\mathrm{cav}} = P_{\mathrm{inc}}t_{\mathrm{rt}}F/\pi, \tag{6}$$

where P_{inc} is the incident power, t_{rt} is the cavity round-trip time, and $F = \pi/T$. The stored energy is 20 μJ just as before. The light intensity at the waist is

$$I_{\mathrm{waist}} = \frac{U_{\mathrm{cav}}/t_{\mathrm{rt}}}{\pi w_0^2}, \tag{7}$$

which is smaller by the ratio $\Delta t_p/t_{\mathrm{rt}}$. I_{waist} is therefore 5.4 $\times 10^4$ W/cm^2. Two observations are worth making. First, because the energy stored in the RDC is the same in the two cases, the ring-down signal will also be the same, with the exception of the 100 MHz time structure in the PS-CRD decay. Second, the peak intensities achieved in PS-CRDS might introduce complications in analysis cased by nonlinear phenomena. On the other hand, short-pulse PS-CRDS might also open avenues for new nonlinear and time-resolved studies using CRDS, particularly in the midinfrared with high powered FELs, or other coherent pulsed light sources.

B. Pulse-stacking conditions

Achieving efficient pulse stacking and high throughput in a RDC is experimentally demanding. We consider briefly each of the conditions cited above for efficient pulse stacking, thus establishing a set of requirements for PS-CRDS experiments. A more detailed discussion can be found elsewhere.[19–22] It is assumed in this discussion that the source pulse train consists of transform-limited Gaussian pulses:

$$E(m)=E_0 e^{ikz} e^{-z^2/2\sigma^2}, \tag{8}$$

where E_0 is the field amplitude, λ is the wavelength, and $k=2\pi/\lambda$. The width of the pulse is indicated by σ.

First we want to estimate the sensitivity of pulse stacking to errors in steering and mode matching. If we define the z axis to be the optical axis of the cavity and we define two planes, $x'y'$ and xy that coincide with the intercept of the z axis with the surface of the mirrors, C_1 and C_2, then we can use Fresnel's approximation of Huygens' integral to compute the field at C_2 in terms of the field $u_{C_1}(x',y')$ at C_1

$$u_{C_2}(x,y)=\frac{-ikl}{L\lambda}\int\int u_{C_1}(x',y')\exp\left[\frac{ik}{2R_1}(x'^2+y'^2)\right]\times\exp\left[\frac{-ik}{2L}\{(x-x')^2+(y-y')^2\}\right]\times\exp\left[\frac{ik}{2R_2}(x^2+y^2)\right]dx'dy'. \tag{9}$$

The integral is over the projection of C_1 on the $x'y'$ plane. To calculate the stacked field this equation is used iteratively to propagate the beam back and forth inside the cavity. If u_n is the profile of the nth incident pulse from the laser source and $\mathbf{D}$ is the propagation operator for the cavity, the the total stored field is

$$u_{\mathrm{total}}(n)=u_n+\sum_{s=1}^{\infty} R^s \mathbf{D}^s u_{n-s}. \tag{10}$$

Calculation of the field is simplified if one assumes a TEM$_{00}$ Gaussian transverse mode profile and uses the infinite mirror approximation. Proceeding to a quantitative analysis of the transverse effects of steering and mode matching, let us assume that the laser beam enters the cavity at C_1 displaced (x_0,y_0) from the cavity optical axis and exits the cavity at C_2 displaced by (x_0',y_0') traveling parallel to the vector $x_0\hat{\mathbf{x}}+y_0\hat{\mathbf{y}}+\hat{\mathbf{z}}$. For small steering errors, the stacked energy can be written

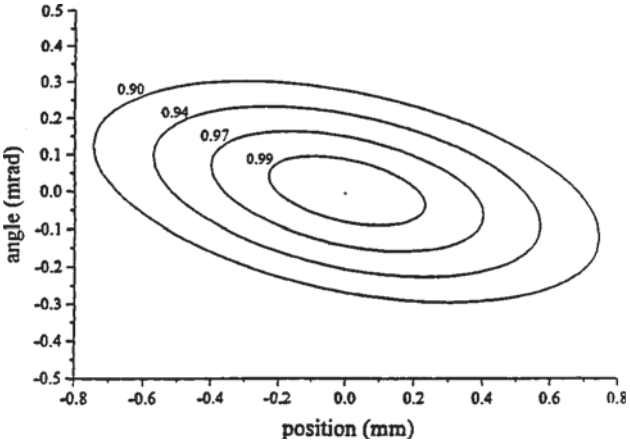

FIG. 2. Acceptance contours for a ring-down cavity of length 2.114 m and mirror radius of curvature 6.0 m. Contours were calculated for normalized stacked energies of 0.99, 0.97, 0.94, and 0.90.

$$U(x_0,x_0')=U_0\exp\left(-\frac{x_0^2}{\Delta x_0^2}-\frac{x_0'^2}{\Delta x_0'^2}-\frac{2x_0x_0'}{\Gamma\Delta x_0'^2}\right), \tag{11}$$

where Γ is a coupling constant with dimensions of length, and the quantities Δx_0 and $\Delta x_0'$ are scaling factors determined by numerical calculations. The calculated cavity acceptance contours are shown in Fig. 2 for the RDC used in our experiments and for normalized stacked energies from 1.0 to 0.90. For a normalized energy of 0.97 we can comfortably take $x_0=150$ μm and $x_0'=150$ μrad as acceptance parameters.

To evaluate the effects of mode matching we parametrize the transverse profile of our TEM$_{00}$ mode using the size of the beam waist, w_0, and the position of that waist, z_0, measured from the front cavity mirror. Calculations show that the RDC is quite tolerant of small mode matching errors. For a normalized stacked energy of 0.97, a beam waist error $\Delta w_0/w_0=16\%$ and a waist position error $\Delta z_0=\pm 81$ cm are allowed.

The stacked field will also be reduced from the value calculated for the ideal case by phase differences between the incident pulses and the intracavity pulse. Phase differences can arise from an actual phase shift of the field within the pulse envelope or a difference in the spacing between incident pulses and the cavity round-trip path length. For a constant length error Δz the stacked energy can be written

$$\frac{U}{U_0}=(1-R)^2\sum_{l=0}^{\infty}\sum_{m=0}^{\infty}R^{l+m}\exp[ik\Delta z(l-m)]\times\exp\left[-\frac{\Delta z^2}{4\sigma^2}(l-m)^2\right]=2\frac{1-R}{1+R}\left[\frac{1}{2}+\sum_{m=1}^{\infty}R^m\cos(m\phi)\exp\left(-\frac{\phi^2m^2}{4k^2\sigma^2}\right)\right], \tag{12}$$

where $\phi = k\Delta z$. As expected, local maxima occur whenever ϕ is an integer multiple of 2π representing constructive intereference between the incident pulses and the intracavity pulse. The amplitude and width of the maxima, however, are different. The maximum at $\phi = 0$ has the largest amplitude and narrowest width. For large finesse, the FWHM of this central maximum is $\Delta\phi = 2\pi/F$. Significant pulse stacking therefore requires the cavity length be set so that $\Delta z \ll 2\pi/(kF)$. With $F = 630$ and a wavelength of 6 μm, the RDC must be set so that $\Delta z \ll 1$ nm. In practice, the cavity length drifts in and out of resonance with the laser source. We must therefore consider the effects of a changing cavity length.

If the length error is not constant, we can define $d\phi/dt = d(k\Delta z)/dt$. Providing that $d\phi/dt \ll \Delta\phi/\tau$, where $\Delta\phi$ is the FWHM of the $\phi = 0$ maximum and τ is the ringdown decay constant, the passage through resonance is adiabatic, i.e., the stacked pulse reaches steady state at each value of ϕ. For the RDC with $F = 2000\pi$, $\Delta\phi/\tau = 71$ rad/s, which corresponds to a cavity length change rate of 68 μm/s at a wavelength of 6 μm. As long as mechanical vibrations of the mirrors produce mirror velocities much less than this value, the stored energy will reach its maximum value as the RDC and the source laser drift through resonance. It should be noted that the requirements on laser source temporal coherence and RDC mechanical stability for PS-CRDS are similar to those of CW-CRDS, with the exception that in CW-CRDS typically only a single longitudinal and transverse mode is excited.

III. EXPERIMENT

The experimental apparatus consists of four separate systems: the high repetition rate source laser, the optical system (including injection optics, RDC, and monochromator), the data acquisition system, and the gas handling system.

A. Source laser

The source laser in the present experiments was the FEL at Stanford. The optical beam from the Stanford FEL consists of a train of picosecond pulses, typically of 1 μJ energy per pulse, repeating at an 11.818 MHz rate. The pulse train continues for several milliseconds and repeats with an overall 5% duty factor. The optical beam quality and stability are exceptional: The beam approaches the transform and diffraction limits and has good position and pointing stability. The spectral and temporal pulse shapes of the FEL beam, continually monitored in a dedicated diagnostic station, are shown in Fig. 3. The center wavelength of the FEL is feedback stabilized to one part in 10^4. The measured position and pointing stability are 30 μm and 2 μrad root-mean-square (rms), respectively.

B. Optical system

The optical system for the ring-down experiment, shown in Fig. 4, includes the beam steering and mode matching optics, the RDC, a monochromator, and a detector. To inject the optical beam into the RDC, two mirrors are provided and arranged to make the four injection coordinates as independent as practical. Mode matching is accomplished with a three-mirror telescope consisting of two 1.0 m radius of curvature (ROC) gold mirrors and one -2.0 m ROC mirror. The RDC is a two-mirror symmetric cavity, 2.115 m in length and enclosed in a vacuum chamber. The cavity length is remotely adjustable by a micrometer and changes in the length are monitored using a linear variable differential transformer located at the base of one of the mirror mounts. The cavity mirrors are high reflectivity dielectric mirrors

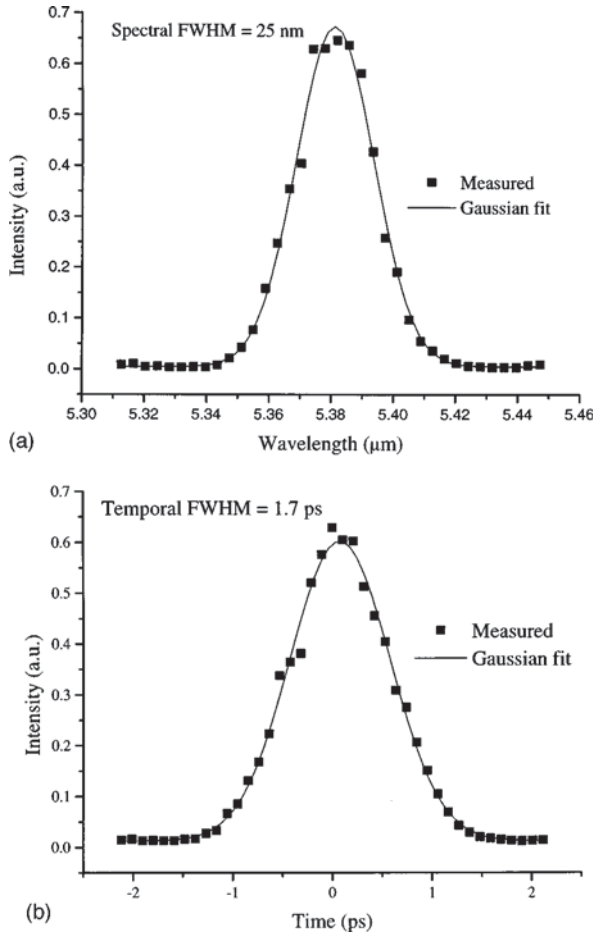

FIG. 3. FEL diagnostics showing (a) laser spectral width, and (b) pulse autocorrelation at 5.38 μm. The measured $\Delta f \Delta t(\mathrm{FWHM}) \approx 0.44$, in agreement with the value calculated for a Gaussian beam.

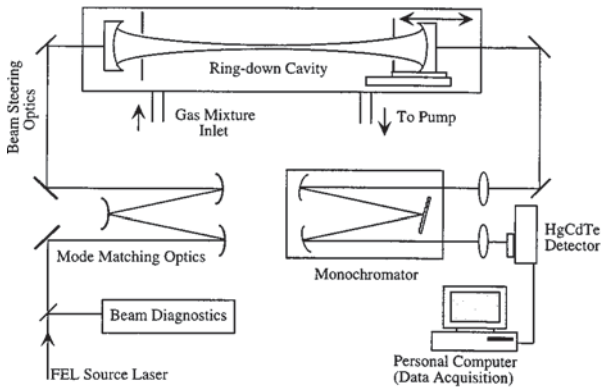

FIG. 4. Experimental setup to perform pulse-stacked cavity ring-down spectroscopy.

coated on silicon substrates (Los Gatos Research), and are planoconvex with a 6.0 m ROC. Cavity alignment is achieved using two remotely controlled picomotors on each mirror. The spectral width of the transform limited 1.7 ps optical pulse provided by the Stanford FEL is 25 nm FWHM. To improve spectral resolution, the optical beam coupled out of the RDC is dispersed in a 1.0 m monochromator (SPEX 1000 M) using a 150 lines/mm grating blazed at 5 μm. The spectrometer output is focused onto a liquid nitrogen-cooled HgCdTe detector (Sensor Physics) that has a noise equivalent power of 3.57×10^{-12} W/$\sqrt{\text{Hz}}$. The detector output is fed to a PC-based data acquisition system.

Alignment of the optical systems was accomplished using a visible HeNe laser beam that had been coaligned to the infrared (IR) beam. The HeNe beam (and therefore the IR beam) was steered to the center of each element of the injection optics and through a pair of pinholes inserted in the RDC mirror mounts. The pinholes define the optical axis of the RDC. Mode matching is less critical, but was accomplished by measuring the transverse size of the beam at several locations using a laser beam diagnostic camera (Spiricon). The pinholes were then removed and the IR beam was focused onto the monochromator input slit with a CaF_2 lens, matching the monochromator f number and maximizing throughput. A throughput of 60% was achieved. To align the RDC optical axis to the axis previously defined by the pinholes, the back mirror of the cavity was inserted first and the back reflection of the IR beam on an aperture was used as a diagnostic to orient the mirror. The front mirror was then inserted and again the back reflection (from the plano surface) on an aperture was used to establish its orientation. Once coalignment of the RDC and pinhole axes was optimized, the cavity length was scanned to achieve pulse stacking. To ensure measurable RDC throughput during the scan, even in the absence of pulse stacking, the IR wavelength was shifted initially to the edge of the mirror reflectivity curve where transmission is significant (5.50 μm). Finally, using the pulse stacked signal as a diagnostic, it was possible to optimize the optical system at the wavelength of interest (5.38 μm).

To proceed quickly with a demonstration of PS-CRDS, several compromises were made in the optics. The most important is the choice of cavity length. The RDC, at 2.115 m, fits conveniently on an optical table, but is only one sixth the length of the FEL optical cavity. An optical pulse is injected into the RDC only once every six optical roundtrips. Thus the effective finesse is reduced by a factor of 6, and the stacked pulse energy by a factor of 36. Despite this reduction, the single shot decay wave forms exhibit good signal-to-noise for stacked pulses. The substantial benefits of pulse stacking are illustrated in Fig. 5. Single shot decay wave forms obtained at 5.50 μm in an evacuated RDC with pulse stacking exhibit an initial signal-to-noise ratio of 300:1. The initial signal-to-noise ratio would have been much larger (3000:1) had we not discarded the first 15 μs of the decay due to the method used to interrupt the FEL optical beam (see discussion below). For comparison, the single shot decay wave form without pulse stacking is also shown in Fig. 5. The initial signal-to-noise ratio here is only 2:1. At 5.50

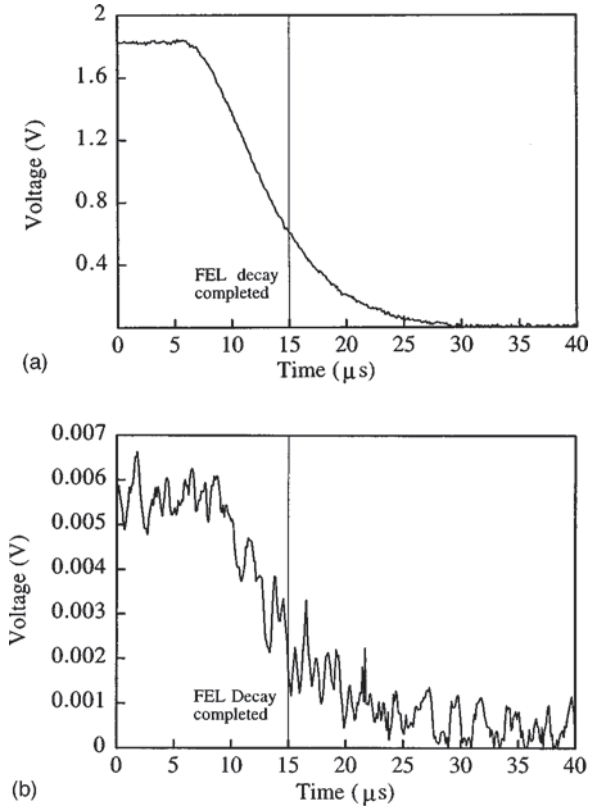

FIG. 5. Single shot ring-down decay waveform obtained with spectrometer slits completely open (a) without pulse stacking, and (b) with pulse stacking.

μm, the decay time constant measured was 7.5 μs, which corresponds to a mirror transmission loss of 940 ppm, and consequently $R=99.9\%$. For these single shot measurements the detector noise was about five to eight times the bit error of the digitization noise.

The use of a single detector at the output of the monochromator, rather than a linear array detector, is a second important compromise. If the sample were a thin film and the absorption line to be studied were greater than the FEL beam spectral width, the breadth of the FEL linewidth would no longer matter. But for measurements of lines that are spectrally narrow, this compromise reduces the data collection rate, perhaps by two orders of magnitude. Finally, the method used to interrupt the FEL optical beam and initiate a ringdown also was compromised: Rather than use an acousto-optic modulator to terminate cleanly the FEL beam, we simply shut off the electron beam from the linac. The decay of the FEL cavity is much faster ($\tau=2.5$ μs) than the RDC, but this expedience forced us to reject the first 15 μs of data in each ringdown. Despite these compromises, we have been able to demonstrate some of the advantages of PS-CRDS.

C. Data acquisition

Ring-down decay wave forms were acquired using a 12-bit, 60 Ms/s digitizer (Gage Applied Sciences: CompuScope 6012). The digitizer scale was adjusted so that the wave form filled as much of the full-scale (±2 V) voltage as possible, in order to achieve maximum vertical resolution. Typically, the digitizer excess noise (e.g., input noise, clock feedthrough,

time base jitter, etc.) equaled one to two bits, leading to an effective vertical resolution of ten to eleven bits.

The digitizer was triggered from the control signal that shuts off the FEL beam (i.e., that terminates the electron beam) with an additional 15 μs delay so that the rapidly decaying FEL cavity output would not interfere with the ring-down decay itself. The wave form acquisition rate ranged from 1 to 10 Hz, with at least 30 pulses building up inside the RDC for each decay wave form. The digitizer output was directly transferred to a computer, and the exponential decays were fit using a Levenberg–Marquardt algorithm with a least-squares prefit of the logarithm of the decay wave form. Total fit times were estimated at about 200 ms on a 266 MHz Pentium processor, running an average of four iterations.

D. Gas handling

Water vapor present in 40% humidity laboratory air was diluted with helium, and the mixture was delivered to the main vacuum chamber by a gas handling system. A capacitance manometer was used to measure the pressure (0.10 to 10 Torr) of a small volume of air (interchangeable between 3.0 and 13.0 m). The air was then delivered to the vacuum chamber, which had been evacuated to a pressure of <1 mTorr. Helium was then added to the vacuum chamber to bring the total pressure to 700 Torr resulting in a partial pressure of H_2O between 500 ppb and 50 ppm.

IV. RESULTS AND DISCUSSION

For the RDC used in this demonstration experiment, the stacked pulse energy can be written

$$U_{\text{stacked}} = (T_1 F_{\text{eff}}^2/\pi^2) U_{\text{inc}}, \tag{13}$$

where T_1 is the transmission through the input mirror and $F_{\text{eff}} = F/6$, accounting for the fact that an FEL pulse is injected into the RDC only once every six optical roundtrips. At 5.38 μm, the decay time constant for the ringdown was measured to be 10.5 μs, making $F = 4680$, assuming $T_1 = \pi/F$. The calculated stacked pulse energy is $41 U_{\text{inc}}$. The stacked pulse energy can also be measured directly. By removing the front mirror of the RDC and measuring the signal after the monochromator, one has established a calibration of the detector with respect to the incident pulse energy. A subsequent measurement of the stacked pulse signal with this detector then gives the stacked pulse energy. The experimentally measured stacked pulse energy was 35 times the incident pulse, within 15% of the calculated value.

The pulse-stacked ring-down measurements described above were performed with the monochromator slits fully open. To make spectrally resolved measurements, the slits were closed to achieve 0.03 nm resolution. Although the resulting single shot decays exhibited a good 30:1 signal-to-noise ratio, oscillations were observed in the wave forms owing to electronic interference. These oscillations were not caused by mode beating. Electronic bandpass filtering was avoided because the sinusoidal pickup on the decay had a period on the same order as the decay constant, so that signal corruption became a concern. Only raw decay wave forms were therefore stored. Mathematical digital bandpass filtering of each shot in the dataset was subsequently performed during data analysis. The filtered decays were fit using the Levenberg–Marquardt algorithm with a linear least-squares prefit. The decays are linear over two decay constants which were measured to be 10.5 μs at 5.38 μm. Because the ring-down decay constant, τ, is given by $\tau = (2L/c)(F/\pi)$; this measurement indicates that for the mirrors used, the power transmission coefficient is 650 ppm at 5.38 μm. It should be noted that the signal-to-noise ratio of single shot ring-down decay wave forms without pulse stacking was less than 1:1, so that single shot decays were no longer visible. Statistics for 90 single shot energy resolved decays are shown in Fig. 6. A Gaussian fit to the histogram gave a standard deviation of 0.2% in τ This 20 ns variation in a 10.5 μs decay constant is equal to the computed fit uncertainty for the individual decays and corresponds almost exactly to the measured rms baseline deviation of 2×10^{-9} cm^{-1}, which determines the system sensitivity at 5.38 μm.

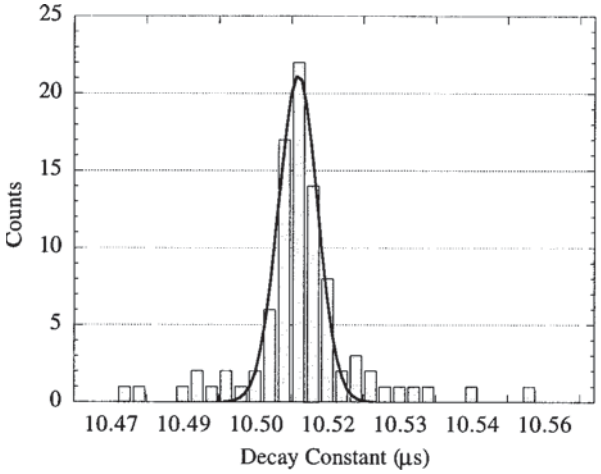

FIG. 6. Histogram of 90 single shot waveforms at 5.38 μm with spectrometer slits closed to 0.03 nm resolution.

PS-CRDS was applied to the spectroscopy of water vapor, which had been pressure broadened to 1 atm with helium. Figure 7 presents a spectrum of a water vapor absorp-

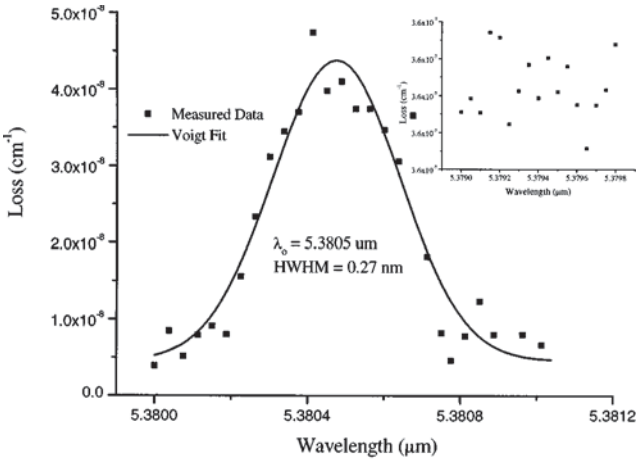

FIG. 7. Spectrum of H_2O diluted in He with fit parameters compared to HITRAN96. This is the $(8,2,6)\rightarrow(9,3,7)$ transition.

tion line having vibrational parameters $(0,0,0)\rightarrow(0,1,0)$ and rotational parameters $(J,K_a,K_c)\rightarrow(J',K_a',K_c')$ equal to $(8,2,6)\rightarrow(9,3,7)$. For a specific rotational line, K_a is the value of $|K|$ for the limiting prolate symmetric top with which the rotation level correlates, while K_c is the value of $|K|$ in the oblate rotor limit. Exact correspondence in line position, and pressure-broadened linewidth with the HITRAN96 database was obtained. Using the HITRAN96 linestrength, a 2 Torr partial pressure of air was computed, a factor of 2 greater than that measured. However, the actual humidity and temperature of the laboratory air were not known with sufficient precision for any conclusions on the absolute moisture content in the cell to be made. From the residual of the line fit computed using parameters from the HITRAN96 database and shown in Fig. 7, a sensitivity of 2.5×10^{-9} cm^{-1} was deduced, which once again agrees with the rms deviation from the baseline measurement of the empty RDC.

V. PERSPECTIVES

Pulse-stacked cavity ring-down spectroscopy can be used with advantage whenever (1) the pulsed light source incident on the ring-down cavity is coherent and has a high repetition rate, and (2) mirrors exist of high reflectance. In this work, we have exploited PS-CRDS using the Stanford FEL to deliver a high-quality optical beam in the midinfrared region. We use high reflectivity dielectric mirrors, which, although expensive, are available at wavelengths as long as 11 μm.

In the original demonstration experiment reported here, a sensitivity of 2×10^{-9} cm^{-1} and a resolution of 0.03 nm was achieved. These do not represent fundamental limitations of the method. We have constructed a 12.392 m long RDC which will increase the absorption path length by a factor of 6 and increase the possible stacked energy by a factor of 36, i.e., a FEL pulse will be injected into the RDC every cavity roundtrip rather than every six. In addition, we will implement a more suitable method of interrupting the FEL source laser beam. With a 10^{-3} power transmission, it is possible, at least in principle, to achieve a stacked energy of 250 μJ (assuming $U_{\mathrm{inc}}=1$ μJ).

CRDS has most often been used in measurements of gases, but possibilities for high sensitivity experiments in thin films also appears interesting. For thin films, the linewidths exceed the spectral width of the FEL pulses and thus spectral analysis of the signal emerging from the RDC will not be necessary. Two possible configurations for thin film experiments are being considered at Stanford: free standing films or films supported by a substrate, inside the RDC, and a three-element RDC exploiting total internal reflection. The film is then ''external'' to the cavity subject only to evanescent fields for studies of weak surface absorption, for example.[24]

Stacking ultrashort pulses also provides an opportunity to explore nonlinear spectroscopy and time resolved spectroscopy. In the RDC cavity under construction, assuming a 250 μJ circulating pulse of Gaussian temporal width 0.64 ps, the peak intensity if 69 GW/cm^2 where Gaussian widths have been used to calculate the area. Thus, the increased signal-to-noise ratio properties of the pulse-stacked system, as well as adding the flexibility of varying the laser polarization, will lend themselves well to studies of very weak or nonlinear phenomena in condensed media. It is envisaged that PS-CRDS will become a new enabling technology for many studies benefitting from absolute and relative absorption measurements.

ACKNOWLEDGMENTS

This work has been supported by the Air Force Office of Scientific Research (Contract No. F49620-98-1-0040) and the Office of Naval Research (Contract No. N00014-94-1-1024).

[1] A. O'Keefe and D. A. G. Deacon, Rev. Sci. Instrum. **59**, 2544 (1988).
[2] P. Zalicki and R. N. Zare, J. Chem. Phys. **102**, 2708 (1995).
[3] D. Romanini and K. K. Lehmann, J. Chem. Phys. **99**, 6287 (1993).
[4] G. Meijer, M. G. H. Boogaarts, and A. M. Wodtke, Chem. Phys. Lett. **217**, 112 (1994).
[5] J. J. Scherer and D. J. Rakestraw, J. Chem. Phys. **107**, 6196 (1997).
[6] J. T. Hodges, J. P. Looney, and R. D. vanZee, Appl. Opt. **35**, 4112 (1996).
[7] D. Romanini, A. A. Kachanov, N. Sadeghi, and F. Stoeckel, Chem. Phys. Lett. **264**, 316 (1997).
[8] B. A. Paldus, J. Martin, J. Xie, J. S. Harris, and R. N. Zare, J. Appl. Phys. **82**, 3199 (1997).
[9] R. Engeln and G. Meijer, Chem. Phys. Lett. **262**, 105 (1996).
[10] R. Engeln and G. Meijer, Rev. Sci. Instrum. **67**, 2708 (1996).
[11] D. Romanini, A. A. Kachanov, N. Sadeghi, and F. Stoeckel, Chem. Phys. Lett. **270**, 538 (1997).
[12] B. A. Paldus, C. C. Harb, T. G. Spence, B. Willke, J. Xie, J. S. Harris, and R. N. Zare, J. Appl. Phys. **83**, 3991 (1998).
[13] T. Kulp (private communication).
[14] J. Faist, C. Gmachl, F. Capasso, C. Sirtori, D. L. Sivco, J. N. Baillargeon, and A. Y. Cho, Appl. Phys. Lett. **70**, 2670 (1997).
[15] S. W. Sharpe, J. F. Kelly, J. S. Hartman, C. Gmachl, F. Capasso, D. L. Sivco, J. N. Baillargeon, and A. Y. Cho, Opt. Lett. **23**, 1396 (1998).
[16] J. T. Hodges, J. P. Looney, and R. D. van Zee, J. Chem. Phys. **105**, 10278 (1996).
[17] S. E. French, D. J. W. Brown, D. S. Knowles, and J. A. Piper, Appl. Opt. **37**, 536 (1998).
[18] V. L. Kalashnikov, V. P. Kalosha, and V. P. Mikhailov, Zh. Prikl. Spektrosk. **58**, 312 (1993).
[19] T. I. Smith, P. Haar, and H. A. Schwettman, Nucl. Instrum. Methods Phys. Res. A **393**, 245 (1996).
[20] T. I. Smith, P. Haar, and H. A. Schwettman, Nucl. Instrum. Methods Phys. Res. A **358**, 319 (1995).
[21] P. Haar, H. A. Schwettman, and T. I. Smith, Nucl. Instrum. Methods Phys. Res. A **358**, ABS40 (1994).
[22] P. Haar, H. A. Schwettman, and T. I. Smith, Nucl. Instrum. Methods Phys. Res. A **A331**, 621 (1992).
[23] K. K. Lehmann and D. Romanini, J. Chem. Phys. **105**, 10263 (1996).
[24] A. C. R. Pipino, J. W. Hadgens, and R. E. Huie, Chem. Phys. Lett. **280**, 104 (1997).